Volume 16, Number 3, 2023. pp. 373-380

Jordan Journal of Physics

ARTICLE

Annealing Effect on Nickel Oxide Nanoparticles Properties

Suhad A. Hamdan

Physics Department, College of Science, University of Baghdad, Al-Jadiriyah, Iraq.

Doi: https://doi.org/10.47011/16.3.12

Received on: 20/11/2022; *Accepted on: 09/01/2023*

Abstract: Sodium hydroxide and nickel chloride have been used in the effective chemical precipitation process to create nickel oxide (NiO) NPs. We investigate how the morphological, structural, magnetic, and optical characteristics of nanocrystalline NiO are affected by annealing at temperatures of 300, 400, and 500 °C. Field emission scanning electron microscope (FE-SEM), X-ray diffractometer (XRD), vibrating sample magnetometer (VSM), and ultraviolet-visible (UV-vis) spectrophotometer have been utilized in order to characterize NiO-NPs. XRD pattern indicates the material's excellent crystallinity. At the same time, the FESEM study of the synthesized samples reveals that the annealing temperature has a considerable impact on the films' surface morphology. The average crystallite size of NiO samples falls within the range of 29–30.9 nm., whereas the average grain size of synthesized NiO-NPs, as determined by FESEM images, is between 25 and 29.6 nm. We demonstrate that as the annealing temperature rises, grains' average size increases, but their shape remains spherical. In addition to that, the UV-Vis spectroscopy analysis shows the particles' significant absorption peak in the UV region. Our investigation reveals that the synthesized samples have direct band gaps. Before annealing, the energy gap measures 2.4 eV; however, by raising the annealing temperature, we were able to attain a broader range of band gap energies for NiO-NPs, with values spanning between 4.05 and 4.95 eV. The created NiO-NPs demonstrate superparamagnetic behavior, which was found in the VSM results examination.

Keywords: Nickel oxide nanoparticles, Annealing, Chemical precipitation, Magnetic properties.

1. Introduction

NiO is a significant transition metal oxide characterized by a stable wide direct band-gap (3.56 eV), a cubic lattice structure, weak absorption bands, and p-type semiconducting activity. NiO thin films present appealing materials that may be employed as functional sensor layers for antiferromagnetic layers, chemical sensors, p-type layers for UV detectors, as well as active electrodes in electrochromic devices and electrochromic devices [1–5]. Nanosized NiO materials can exhibit both superparamagnetic and superantiferromagnetic properties [4]. Due to their potential for use in a number of applications, including gas sensors [9], battery cathodes [10, 11], catalysis [12], and electrochromic films [13], NiO-NPs have gained growing attention. Various synthesis techniques have been explored for the production of NiO-NPs, including precipitation [14] solvothermal process [15], as well as microwave [16-18], hydrolysis precipitation [19], hydrothermal [20], and sol-gel technique [21] approaches.

In a process called the sol-gel approach, followed by the heat treatment, Gao *et al*. have synthesized the NiO-NPs and nanotubes. In this experiment, the researchers observed ferromagnetic properties at room temperature, characterized by non-zero coercive fields and

Corresponding Author: Suhad A. Hamdan **Email**: Suhadah22@gmail.com

hysteresis loops. [22]. Kemary *et al*. have described NiO-NPs synthesis through chemically reducing nickel chloride with hydrazine at room temperature and thermally decomposing precursor nickel hydroxide NPs [23]. NiO-NPs with diameters ranging from 3.5 to 12.4 nm have been synthesized through the thermal decomposition of nickel acetate at various temperature degrees in salt solutions of Li_2CO_3 and NaCl, according to a paper by Duan *et al*. [24]. Mohammadyani *et al*. have used a quick microwave-assisted approach to rapidly synthesize and analyze NiO-NPs, utilizing a microwave-improved homogeneity and reduced mean particle size in NiO powder that was created [25].

In 2021, E. J. Vishaka *et al*. synthesized pure nickel oxide (NiO) nanoparticles from nickel acetate by co-precipitation method. Their findings indicated that the average size of NiO nanoparticles was 30.1052 nm. Additionally, their investigation of the PL in the NiO nanoparticles revealed the blue and green emissions. Furthermore, their UV-vis spectra analysis showed the absorption edges corresponding to NiO at 327 nm [26].

By using a sol-gel combustion synthesis technique, Tadic *et al*. have created NiO-NPs that were dispersed in an amorphous silica matrix. The sample was then analyzed. The NPs were spherical and had a narrow particle size range with an average size of approximately 5 nm. The magnetization measurements identified two maxima at 5^oK and 56^oK in the zero-field cooled curve of magnetization. The researchers have come to the conclusion that NiO-NPs' small size and crystal lattice flaws are to blame for their magnetic characteristics. NiO-NPs' magnetic characteristics are highly dependent on their crystal structure, size, and morphology [27]. The first study on NiO's size-dependent magnetic characteristics was published by Richardson *et al.* [28]. Extensive research has been conducted on the relationship between a particle size and its magnetic characteristics [29, 30].

There are several challenges involved in comparing the magnetic behavior of a sample containing NPs of various sizes. These challenges include variations in the sample's density as particle size changes, fluctuations in particle size with temperature variations, and alterations in the structural properties of the particles as their size changes. However, it has been noticed that as particle size decreases, the saturation magnetization for magnetic materials also decreases. This phenomenon restricts the use of nanostructured magnetic materials in magnetic recording [31]. The decrease in saturation magnetization in nanostructured magnetic materials has been attributed to the presence of non-magnetic layers on the surfaces of the tiny particles. Additionally, this effect can be compounded by the existence of even finer particles in the superparamagnetic range [31, 32].

In the present study, NiO-NPs films were prepared by using the chemical precipitation technique and annealed at temperatures of 300, 400, and 500 °C. The purpose of this work was to examine how the annealing temperature affects the morphological, structural, magnetic, and optical properties of the synthesized NiO nanostructures.

The structure related to the NiO nanostructures was analyzed with the help of the Shimadzu 6,000 XRD system and the intensity is recorded as a Bragg angle function. We employed Cu (Kα) with λ= 1.5405 Å wavelength as the radiation source. For the voltage and current settings, values of 40 kV and 30 mA were used, respectively. The scanning angle 2θ was varied between 20 and 60 degrees, at a speed of 4 degrees per minute, with a preset time of 0.24 seconds. For analyzing the morphology of the samples, a FESEM was used (MIRA3 model-TE-SCAN, Dey Petronic Co.). To investigate the optical characteristics of the prepared thin films, including absorbance-based absorbance spectra and optical energy gaps, a UV-visible spectrophotometer (Meterrech SP – 8001 with a wavelength of 190-1100 nm) was utilized. In addition, the optical energy bandgap was determined using the Tauc relation method. During magnetic experiments with the use of a VSM, M-H curves were recorded for the samples using an AGFM-VSM model 117.

2. Experimental Methods

The chemical precipitation process was used to create NiO-NPs. Both the necessary concentrations of NaOH and $NiCl_2.6H_2O$ aqueous solutions were dissolved separately in distilled water. The NaOH solution has been added dropwise to the $NiCl_2.6H_2O$ solution while stirring. The resultant solution was stirred

at a temperature of 80°C for five hours. To remove the unreacted salts, the resultant green solution was filtered through filter paper, washed once with ethanol, three times with distilled water, and finally once with acetone. After that, it was dried in a hot air oven for four hours at 100 °C . Using a pestle and mortar, the dried $Ni(OH)_2$ material was ground into powder. This acquired dried powder was annealed at temperatures of 300, 400, and 500 °C for 4 h to produce powder that is NiO-NPs in a black color.

3. Results and Discussion

In Fig. 1, the NiO powders synthesized at various annealing temperatures are depicted with their XRD patterns. Polycrystalline is visible in XRD patterns. The amorphous silica matrix is responsible for the broad peak which could be seen at 2θ = 25°; the other peaks emerge nearby at 2θ = 35° and 43°, corresponding to 111 and 200 planes. The cubic structure of NiO is well-allocated to such peaks (space group Fm3/m; a = 4.176Å; JCPDS 78-0423). With the use of the Debye-Scherrer equation, the average crystallite size (D_{ave}) of NiO may be determined [33]:

$$D = k\lambda/\beta\cos\theta \quad (1)$$

where θ stands for the angle of Bragg's diffraction, λ denotes Cu-Kα radiation wavelength, k represents constant (approximately 0.9), and β is FWHM peak intensity.

The estimated average crystallite sizes of the samples that were annealed at temperatures of 300, 400, and 500 °C were 29.12, 30.89, and 30.91 nm, respectively. This indicates that when temperature rises, crystallite size somewhat increases. This behavior was anticipated since heating promotes particle diffusion and agglomeration [34–36]. Since the crystallite size will be huge at higher temperatures, the diffraction peaks will become stronger. This is promoted by thermally induced crystallite growth [37].

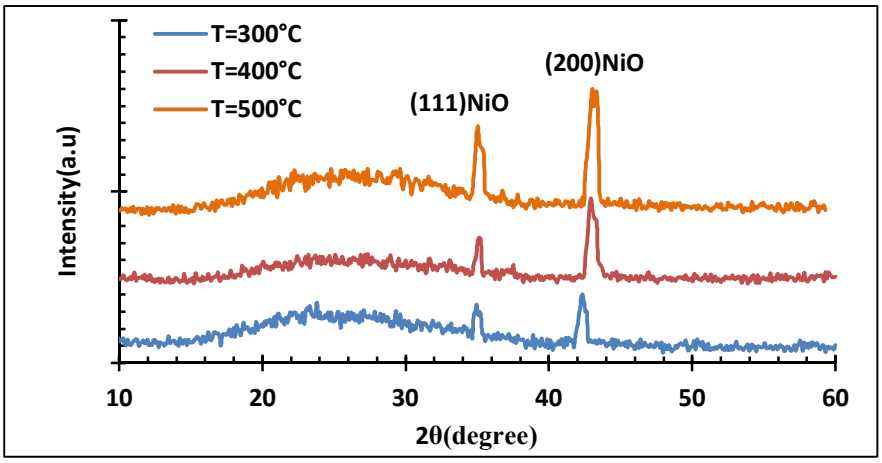

FIG. 1. XRD patterns of NiO-NPs that have been prepared at various temperatures of annealing.

The samples' particle size and surface texture have been examined by using morphology analysis. Magnified FESEM images of NiO-NPs are depicted in Fig. 2. The findings show that the agglomeration process has caused the particles to take on a spherical shape and form nanoclusters. According to [38–42], the average NiO-NP grain sizes for samples that were annealed at 300, 400, and 500 °C, were 25.903, 27.802, and 29.642 nm, respectively. Our XRD pattern showed that as the temperature rises, the grain size increases. Particle sizes have increased and grain agglomeration has occurred at temperatures up to 500 °C.

UV-visible absorption measurements were conducted using the solution, and Fig. 3 presents the UV-visible absorption spectra of the NiO-NPs. As can be seen, the absorbance regarding NiO-NPs was found to be connected to the UV region in the 230–317 nm range, and absorbance values decreased as the annealing temperature was raised. In general, NPs showed a modest absorption in the UV region because of their growing particle size and decreasing surface area [43]. NiO-NPs, on the other hand, have a larger surface area and a small size, which allows them to demonstrate a strong ability to efficiently receive photons and show intense absorption [44].

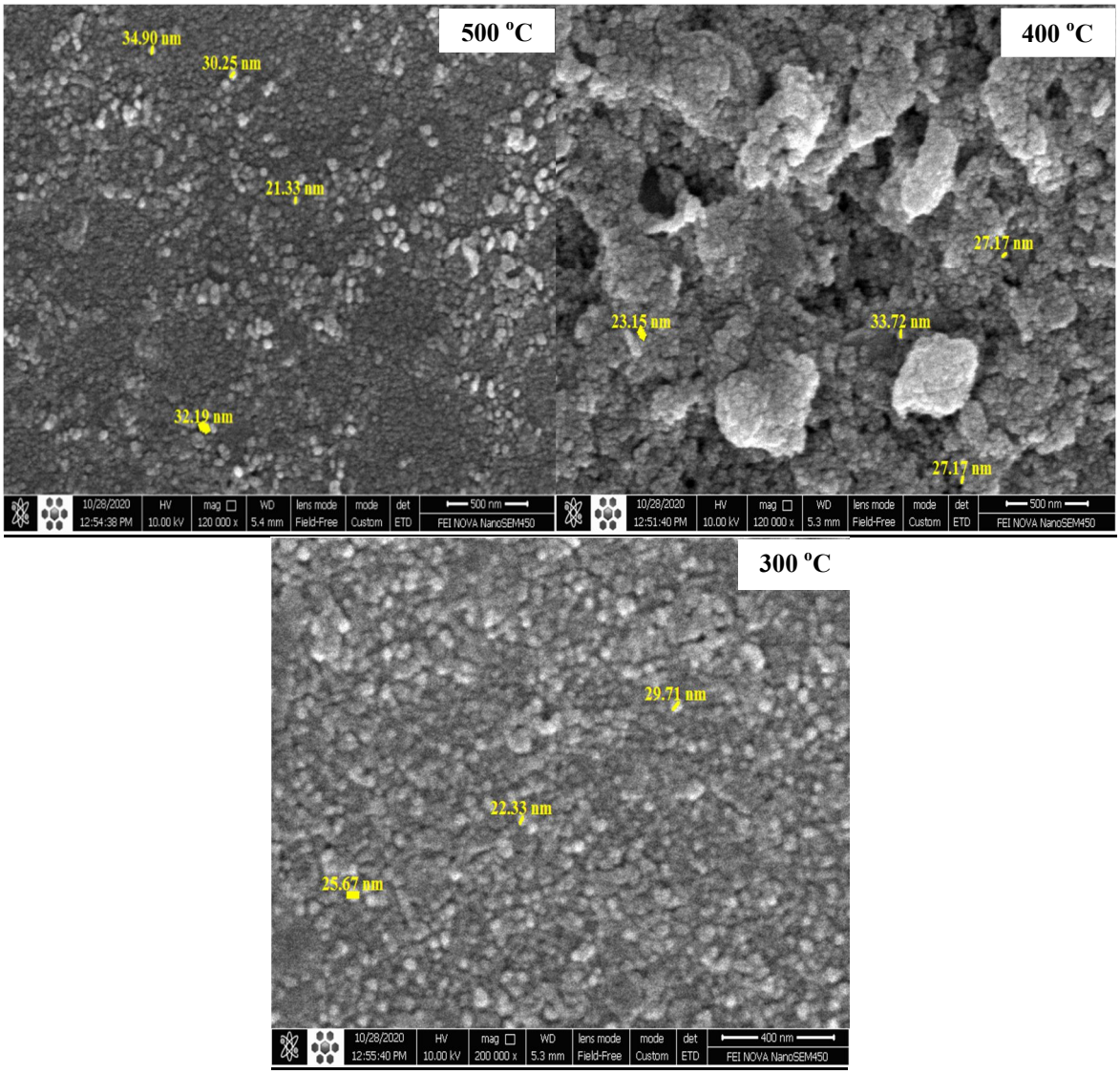

FIG. 2. FESEM images of NiO-NPs at different annealing temperatures.

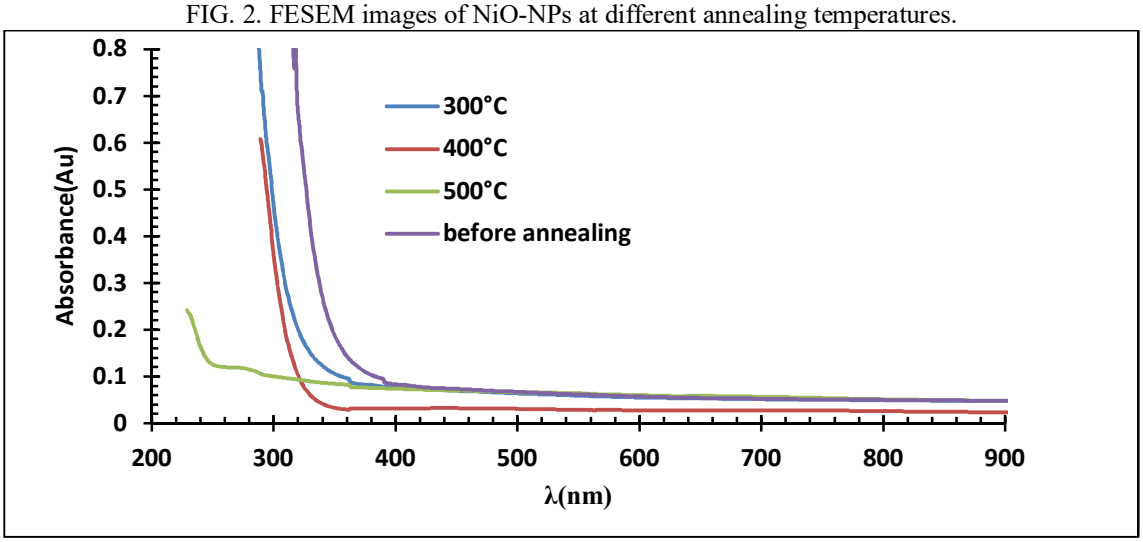

FIG. 3. UV-Vis absorption spectra NiO-NPs.

When compared to the edge of the absorption of bulk NiO, which is at about 340 nm, it could be noticed that the sharpest absorption edge of NiO-NPs appears at roughly 288nm [45]. This results from the quantum confinement effect. With the use of the well-known Tauc relation,

we specified the energy band gap of NiO-NPs [33].

$$(\alpha h\nu)^n = A\,(h\nu - E_g) \quad (2)$$

where hν denotes the photon energy, α represents the absorption coefficient, E_g stands for the optical band gap, A denotes absorbance, and n signifies the number characterizing the nature of the transition process. For indirect transition n = 1/2, whereas for the direct transition n = 2.

As a result, projecting the linear section of $(\alpha h\nu)^2$ Vs h ν curve to the energy axis, as illustrated in Fig. 4, will yield the optical band gap for the absorption edge. The sample's energy gap value before annealing is 2.4 eV. However, with annealing temperatures of 300, 400, and 500 °C, the corresponding band gap energy values obtained from this curve changed to 4.05, 4.08, and 4.97 eV. These band gap energy values obtained after annealing significantly exceed the 3.65eV band gap of bulk NiO [45, 46].

Therefore, it was proven that NiO particles that have been synthesized are nanoscale. The energy band gap is shown to expand with annealing and the reduced defects caused by annealing temperature lead to modest changes in shorter wavelengths [47].

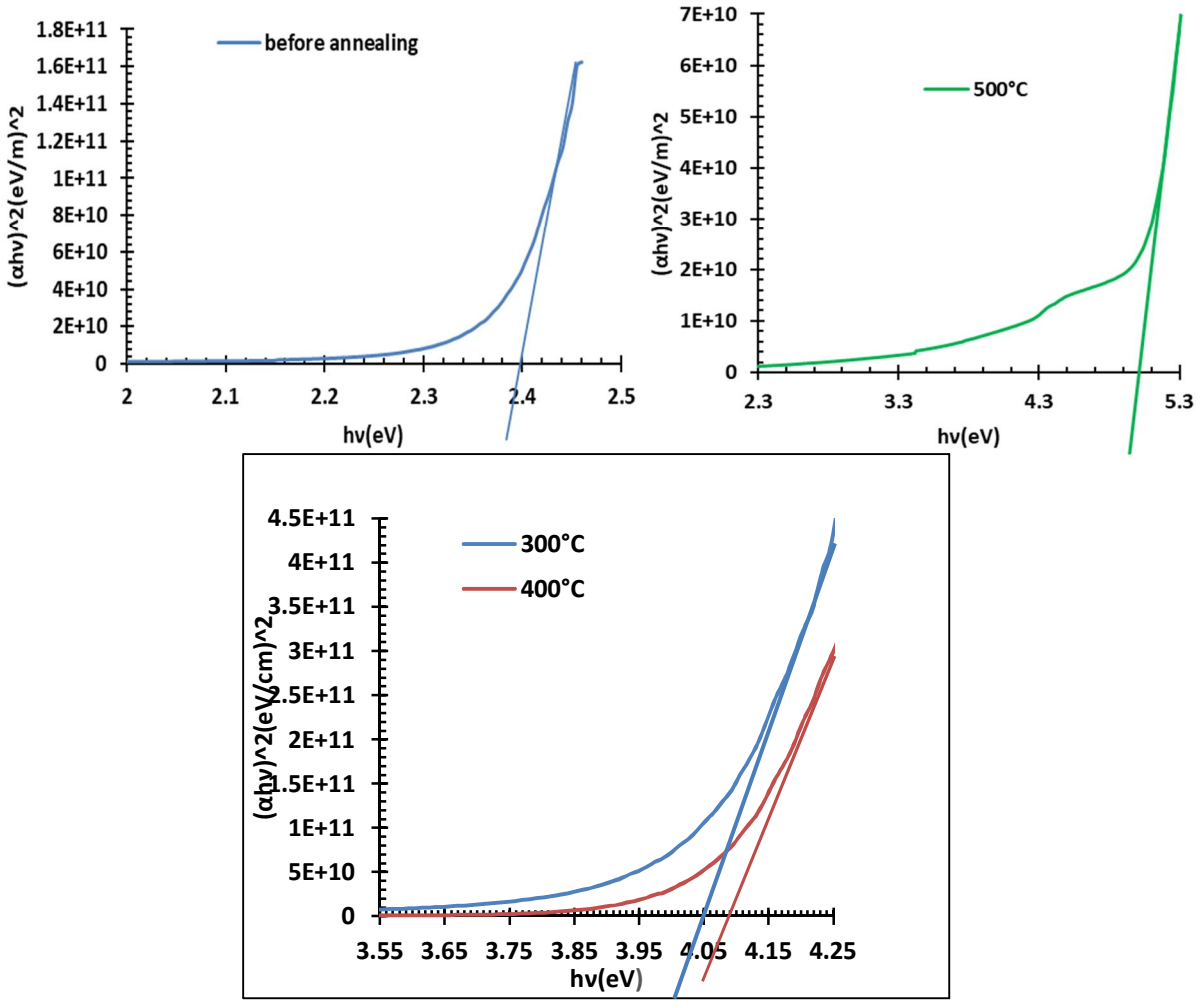

FIG.4. Plot of Tauc relation for NiO-NPs.

TABLE 1. Results from UV–Vis analysis and bandgap E_g of NiO-NPs.

Temperature(°C)	$\lambda_{max.}$ (nm)	Absorbance	E_g (eV)
Before annealing	317	0.708	2.4
300	288	0.798	4.05
400	287	0.632	4.08
500	230	0.237	4.97

The VSM analysis was performed in order to look into the magnetic characteristics of synthesized NiO-NPs at 300, 400, and 500 °C. Figure 5 shows the magnetization M curve of the synthesized NiO-NPs in relation to the applied magnetic field H. Table 2 presents several metrics, including remanent (Mr), magnetism saturation (Ms), and coercivity (Hc). As the temperature rises, the magnetic parameters become less effective.

Due to the lack of hysteresis, remanent magnetization (Mr), and coercive force (Hc), the synthesized NiO-NPs exhibited superparamagnetic behaviors [48]. The prepared NPs' low saturation magnetization, as compared to the bulk form of the NiO (54 emu/g), could be related to the impacts of NP size, which could lower the magnetization [49]. The results of the FESEM and XRD have also shown a decrease in particle size. The process of making NiO-NPs might result in a decrease in particle size and exhibit superparamagnetic behavior [50, 51]. Additionally, this superparamagnetic behavior might be caused by structural flaws that resulted in an oxygen gap from thermal processes that led to interactions between bound magnetic polarons (BMPs) [52]. The results have been in agreement with the studies of Bharathy and Raji [53] and Suresh *et al.* [54].

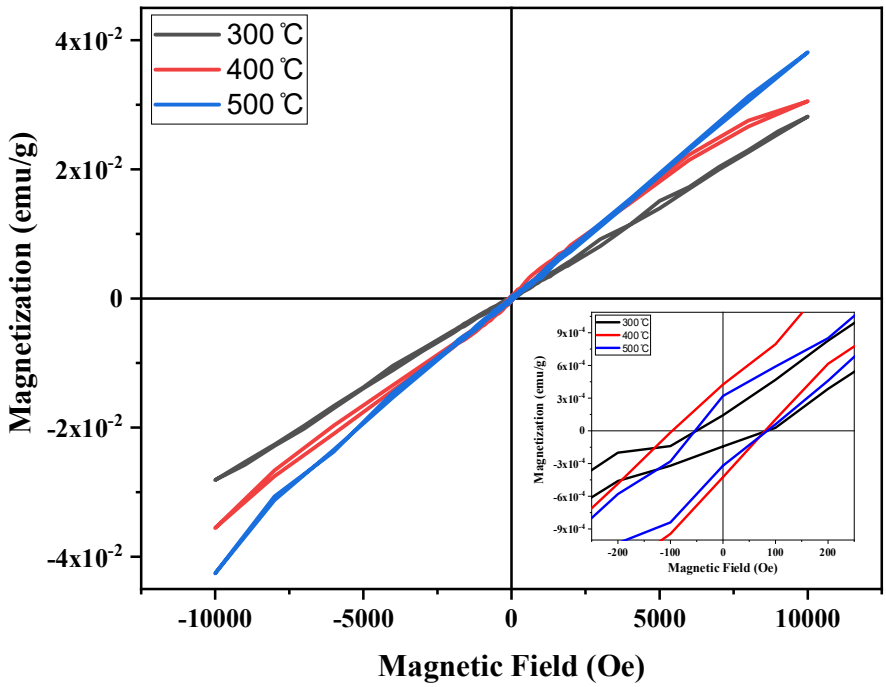

FIG. 5. M-H curves for NiO- NPs annealing at temperatures of 300, 400, and 500 °C.

TABLE 2. Magnetic parameters for NiO NPs annealing at temperatures of 300, 400, and 500 °C.

Annealing temperature (°C)	Ms (memu/g)	Mr (memu/g)	Hc (Oe)
300	2.82	0.144	50.59
400	3.05	0.417	96.14
500	3.81	0.313	53.34

4. Conclusion

Efficient synthesis of nanostructured NiO particles was achieved through chemical precipitation. Extensive investigations were conducted to explore the chemical and physical properties of these nanoparticles. The nanocrystalline nature of the synthesized particles was confirmed by the XRD data, and it was discovered that the crystallite size increases with higher annealing temperatures. Synthesized NPs had a spherical form and an average particle size of between 25 and 29 nm, according to the FESEM examination. UV-visible absorption studies revealed that the synthesized samples exhibited a higher band gap compared to NiO before annealing and in bulk. Furthermore, it was observed that an increase in annealing temperature causes a blue shift in absorption spectra. Due to the reduced dimensions of the synthesized samples, their superparamagnetic characteristics were investigated using VSM analysis.

References

[1] Hong, S.J., Mun, H.J., Kim, B.J. and Kim, Y.S., Micromachines, 12 (2021) 1168.

[2] Baran, S., Hoser, A., Penc, B. and Szytula, A., Acta Phys. Pol. A, 129 (2016) 35.

[3] Verma, V. and Katiyar, M., Thin Solid Films, 527 (2013) 369.

[4] Shaaban, E.R., Kaid, M.A. and Ali, M.G.S., J. Alloys. Comp., 613 (2014) 324.

[5] Soleimanpour, A.M., Hou, Y. and Jayatissa, A.H., Sens. Actuators, B-Chem., 182 (2013) 125.

[6] Grilli, M.L., Sarcina, I.D., Bossi, S., Rinaldi, A., Pilloni, L. and Piegari, A., Thin Solid Films, 594 (2015) 261.

[7] Gowthami, V., Meenakshi, M., Perumal, P., Sivakuma, R. and Sanjeeviraja, C., Mater. Sci. Semicond. Process., 27 (2014) 1042.

[8] Karpinski, A., Ouldhamadouche, N., Ferrec, A., Cattin, L., Richard-Plouet, M., Brohan, L., Djouadi, M.A. and Jouan, P.-Y., Thin Solid Films, 519 (2011) 5767.

[9] Dooley, K.M., Chen, S.Y. and Ross, J.R., J. Catal., 145 (1994) 402.

[10] Yang, H.X., Dong, Q.F. and Hu, X.H., J. Power Sources, 79 (1999) 256.

[11] Hotový, I., Huran, J., Spiess, L., Čapkovic, R. and Haščıḱ, Š., Vacuum, 58 (2000) 300.

[12] Miller, E.L. and Rocheleau, R.E., J. Electrochem. Soc., 144 (9) (1997) 3072.

[13] Wang, G., Lu, X., Zhai, T., Ling, Y., Wang, H., Tong, Y. and Li, Y., Nanoscale, 4 (10) (2012) 3123.

[14] Gajengi, A.L., Sasaki, T. and Bhanage, B.M., Catal. Commun., 72 (2015) 174.

[15] Anandan, K. and Rajendran, V., Mater. Sci. Semicond. Process., 14 (1) (2011) 43.

[16] Zhang, G., Chen, Y., Qu, B., Hu, L., Mei, L., Lei, D., Li, Q., Chen, L., Li, Q. and Wang, T., Electrochim. Acta, 80 (2012) 140.

[17] Nasseri, M.A., Kamali, F. and Zakerinasab, B., RSC Adv., 5 (2015) 26517.

[18] Behnajady, M.A. and Bimeghdar, S., Chem. Eng. J., 239 (2014) 105.

[19] Danial, A.S., Saleh, M.M., Salih, S.A. and Awad, M.I., J. Power Sources, 293 (2015) 101.

[20] Zheng, Y.-Z., Ding, H.-Y. and Zhang, M.-I., Res. Bull., 44 (2) (2009) 403.

[21] Ling, S., Nheu, L., Dai, A., Guo, Z. and Komesaroff, P., Int. J. Cardiol., 128 (2008) 350.

[22] Gao, H., Gao, D., Zhang, J., Zhang, Z., Yang, G., Shi, Z., Zhang, J., Zhu, Z. and Xue, D., Micro Nano Lett., 7 (2012) 5.

[23] El-Kemary, M., Nagy, N. and El-Mehasseb, I., Mat. Sci. Semicon. Proc., 16 (2013) 1747.

[24] Duan, W.J., Lu, S.H., Wu, Z.L. and Wang, Y.S., J. Phys. Chem. C, 116 (2012) 26043.

[25] Mohammadyani, D., Hosseini, S.A. and Sadrnezhaad, S.K., Int. J. Mod. Phys., 5 (2012) 270.

[26] Vishaka, E.J., Priya Dharshini, M., Shallyb, V. and Gerardin Jayam, Sr., Jordan J. Phys., 14 (5) (2021) 409.

[27] Tadic, M., Nikolic, D., Panjan, M. and Blake, G.R., J. Alloy. Comd., 647 (2015) 1061.

[28] Richardson, J.T. and Milligan, W.O., Phys. Rev., 102 (1956) 1289.

[29] Kodama, R.H., Makhlouf, S.A. and Berkowitz, A.E., Phys. Rev. Lett., 79 (1997) 1393.

[30] Winkler, E., Zysler, R.D., Mansilla, M.V. and Fiorani, D., Phys. Rev. B, 72 (2005) 132409.

[31] Che, S., Wang, J. and Chen, Q., J. Phys. Condens. Mater., 15 (2003) L335.

[32] Maaz, K., Mumtaz, A., Hasanain, S.K. and Ceylan, A., J. Magn. Magn. Mater., 308 (2007) 289.

[33] Abd Karem, I.K. and Hamdan, S.A., Iraqi J. Sci., 63 (6) (2022) 2482.

[34] Ghoneim, N.M., Hanafi, S. and Abo El-enein, S.A., J. Mater. Sci., 22 (1987) 791.

[35] Cabot, A. *et al*., Electrochem. Solid State Lett., 7 (2004) G93.

[36] Lu, J. and Fang, Z.Z., J. Am. Ceramic Soc., 89 (2006) 842.

[37] Sheena, P.A. *et al*., Nanosyst.: Phys. Chem. Math., 5 (3) (2014) 441.

[38] Rahdar, A., Aliahmad, M. and Azizi, Y., J. Nanostructures, 5 (2015) 145.

[39] Khalaji, A.D., J. Ultrafine Grained Nanostruct. Mater., 48 (1) (2015) 1.

[40] Ganachari, S.V., Bhat, R., Deshpande, R. and Abbaraju, V., Recent Res. Sci. Technol., 4 (4) (2012) 50.

[41] Shanaj, B.R. and John, X.R., J. Theor. Comput. Sci., 3 (2) (2016) 1000149.

[42] Srikanth, R., Int. J. Chem. Tech. Res., 10 (5) (2017) 145.

[43] Vijayakumar, S., Krishnakumar, C., Arulmozhi, P., Mahadevan, S. and Parameswari, N., Microb. Pathog., 116 (2018) 44.

[44] Kaewmuang, P., Thongtem, T., Thongtem, S., Kittiwachana, S. and Kaowphong, S., Russ. J. Phys. Chem. A, 92 (2018) 1777.

[45] Deshpande, M.P., Patel, K.N., Gujarati, V.P., Patel, K. and Chaki, S.H., Adv. Mat. Res., 1141 (2016) 65.

[46] Sabouri, Z., Akbari, A., Hosseini, H.A., Hashemzadeh, A. and Darroudi, M., J. Clust. Sci., 30 (6) (2019) 1.

[47] Jeyaseelan, S.C., Kumar, R.P., Kaviyarasu, K. and Benial, A.M.F., J. Mol. Struct., 1197 (2019) 134.

[48] Manikandan, A., Vijaya, J.J. and Kennedy, L.J., Phys. E, 49 (2013) 117.

[49] Torki, F. and Faghihian, H., Photochem. Photobiol., 94 (2018) 491.

[50] Anandan, K. and Rajendran, V., Mater. Sci. Eng. B, 199 (2015) 48.

[51] Taghizadeh, F., Opt. Photonics J., 6 (2016) 164.

[52] Bi, H., Li, S., Zhang, Y. and Du, Y., J. Magn. Magn. Mater., 277 (2004) 363.

[53] Bharathy, G. and Raji, P., Physica B: Condens. Matter., 530 (2018) 75.

[54] Suresh, R., Ponnuswamy, V., Sankar, C., Maniekam, M., Venkatesan, S. and Perumal, S., J. Magn. Magn. Mater., 411 (2017) 787.